DESIGN OF A 320 kV ION ACCELERATOR FOR MULTIPLY CHARGED HEAVY IONS

J.G. Bannenberg, A.J.H. Boerboom
FOM-Instituut voor Atoom- en Molecuulfysica, Kruislaan 407, Amsterdam
The Netherlands

Summary

An accelerator for multiply charged ions with a terminal voltage of 320 kV has been developed. A pulsed cold cathode P.I.G. ion source with titanium cathodes and side extraction is immersed in a magnetic field, to analyze and focus the beam into the entrance aperture of the post accelerating column. Matrix calculations of the ion optics are given. After the accelerator the beam can be focussed with an electrostatic triplet into a gascell. The charge exchanged beam is analyzed in a magnet provided with several exit gates for the respective charge states.

Introduction

The influence of the charge state of a projectile particle in inelastic collision processes is a relatively inexplored field in atomic physics. Collisions with a projectile that is ionized in an inner shell give rise to a radiative transfer in the short lived quasi molecule[1]. Inner shell excitations in ion-solid state collisions are observed, not occurring in a gas target. These can be explained only by a high charge state of the projectiles in the solid state.

These types of processes can be studied however in a single collision in the gasphase by the use of multiply charged ions with a helium-like or hydrogen-like electron configuration of atoms from the first row of the periodic system and fluor-like configurations from the second row. The use of these beams in the energy range from 0.1 - 2 MeV opens up a new field of atomic collision research. This energy range is inaccessible by nuclear physics accelerators whereas at this energy the molecular model is still valid[2].

Ion source design

The ion source design is based on the cold cathode P.I.G. source developed by Wolf out of the Anderson and Clark design[3,4,5]. The arc voltage of a cold cathode discharge is governed primarily by the secondary emission of the cathodes. The use of titanium cathodes limits the arc voltage to about 2 kV. The lifetime of the source depends mainly on the power dissipated in the source, whereas the ion current of high charge state ions at minimized gas flow, rises rapidly with arc current. To limit the power dissipated in the source, the arc is pulsed with a duty cycle between 5% and 50%. The source has the following main dimensions: cathode diameter: 10 mm, distance between cathodes: 58 mm, anode bore: 6 mm, anode slit: 10 × 0.1 mm. The anode is milled from a solid copper block (fig. 1) and has a circular cooling channel arranged at the backside of the anode block. The cathodes are mounted on internally cooled copper blocks, coupled together with a stainless steel bridge. This bridge also serves as an electron dump for electrons moving in trochoidal paths in the $E \times B$ direction, the E-field arising from the extraction field. The source is mounted at the end of a stainless steel tube that acts as a gas reservoir. This reservoir is bolted on to an insulating manifold on which the cooling lines are attached with tube couplings. One ceramic feedthrough mounted on the rectangular source flange is used for a gas inlet tube to the reservoir also serving as a high voltage lead to the anode block. One other ceramic feedthrough connects to the cathode cooling line. The source can be operated at 20 kV positive with respect to the vacuum flange and the extraction electrode. The extraction electrode is cooled with two cooling channels running parallel to the slit. This electrode is protruding inside two ridges on the anode block to create an electric field parallel to the magnetic field to prevent a discharge. The extractor can be moved parallel and perpendicular to the anode face. Both movements are motor-controlled via the telemetry system. The parallel movement is introduced with a lead-screw and a sliding vacuumflange; the other movement via a pair of conical gear-wheels and a lead-screw inside the vacuum. Attached to the extractor are two aluminium plates with a 25 mm gap to obtain space neutralization.

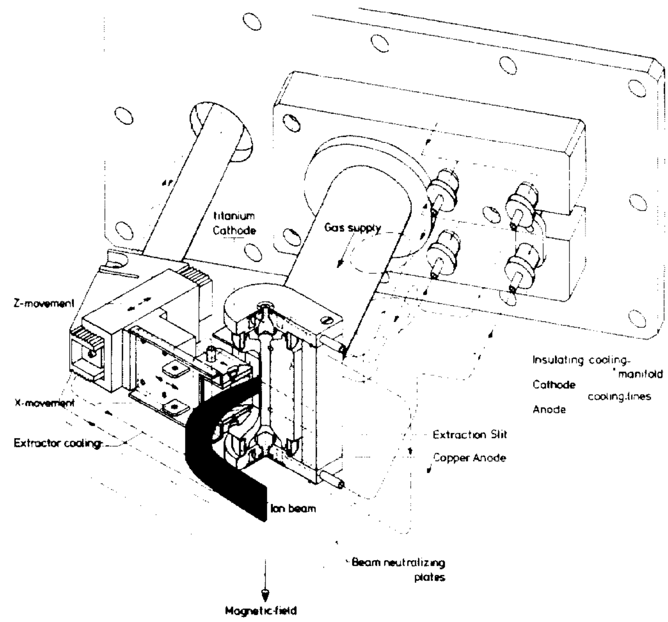

Fig. 1 - P.I.G. Ion source

Source magnet

For a stable P.I.G. discharge a minimum B-field of 2 kGauss is necessary. The large gap (115 mm) necessary to accomodate the source and vacuum chamber walls, limits the maximum field that can be obtained with a reasonable power supply (6 kW) to 5000 Gauss. High voltage is limited to an upper value of 20 kV by the high voltage holding problem in crossed fields and to a lower value of 5 kV by the ion extraction efficiency.

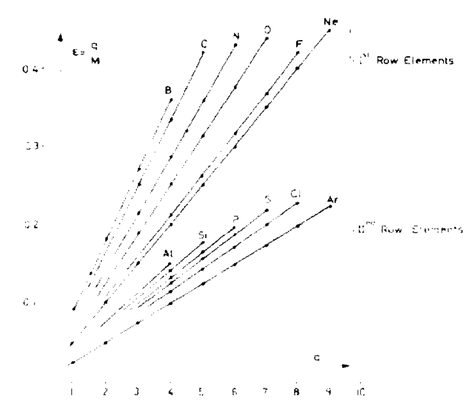

Fig. 2 - Specific charge as a function of charge number.

In fig. 2 are given the ions and charge states that are to be handled by the source and magnet. To analyze these ions a magnetic field given by:

$$B = (144/R)(ME/q^2)^{\frac{1}{2}} \qquad \text{(eq. 1)}$$

is necessary, with B in Gauss, E in eV, R in cm.
Substituting $E = qV$ and $\varepsilon = q/M$ in equation (1) we find:

$$B = (144/R)(V/\varepsilon)^{\frac{1}{2}} \qquad \text{(eq. 2)}$$

For a given radius of curvature and magnetic field, there is a linear relationship between V (extraction voltage) and ε. In Fig. 3 this relationship is sketched for $R = 10$ cm, with B as parameter. A comparison with fig. 2 shows that Ar^{7+} can be handled at 20 kV extraction voltage. The operating limits are marked. A smaller radius would give a cheaper magnet, however the lower limit would rise as indicated, allowing only 11.5 kV extraction voltage for Ar^{7+}.

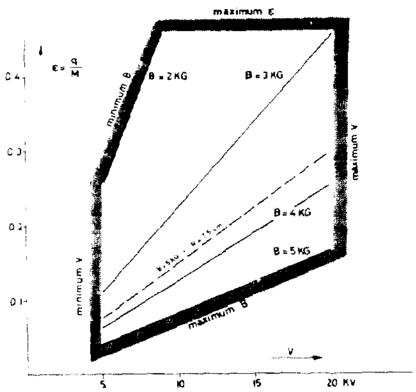

Fig. 3 - Operating region for source and magnet.

The charge state q is proportional to MV/B^2 (eq. 2). An electronic circuit measures V/B^2 and a multiplication factor can be chosen such that a digital meter displays the correct charge number q at the control desk via the telemetry system. One now can change V and/or B in such a way that charge number q + 1 is displayed. The source conditions and/or extractor position can now be varied for maximum ion current of charge q + 1.

The magnet has 230 mm diameter round polepieces, cut at an angle at the beam exit, with hollow copper coils around the poles. A stainless steel T-shaped flat vacuum chamber has 80 mm diameter pieces of soft iron welded on the two opposite flat sides. These pieces fit in 80 mm diameter holes in the two poles and are bolted on the poles to prevent a vacuum-collapse of the chamber.

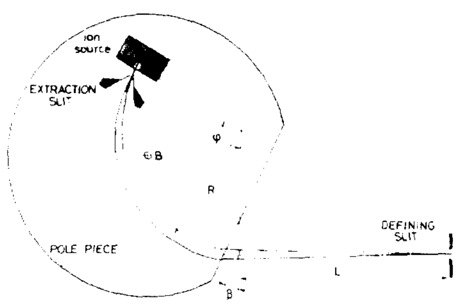

Fig. 4 - Source and magnet ion optics.

Ion optics

Magnet and driftlength. The slit source is immersed (fig. 4) in the magnetic field. We impose the condition that in the radial plane we have point to point imaging and in the axial plane a line to point imaging[6]. We define: angle of deflection ϕ, exit angle β, radius of curvature R and driftlength magnetic edge to image L. There are two independent conditions and two independent variables: ϕ and β. The matrix between source and image can be found by multiplying the matrices for the driftlength, the exit angle and the homogeneous magnetic field[7].

In the product matrix for the radial plane we require that the element $a_{12} = 0$; in the axial plane that the element $b_{11} = 0$. From this can be derived:

$$L = -2R \operatorname{tg} \phi \qquad \text{(eq. 3)}$$

$$\operatorname{tg} \beta = -1/2 \operatorname{tg} \phi \qquad \text{(eq. 4)}$$

So $\phi > 90^o$ and $\beta > 0^o$.

All matrix elements can now be calculated:

Radial matrix: $M_a =$ (eq. 5a)

$$\begin{pmatrix} 2\cos\phi & 0 & 2R(\cos\phi - 1)/\cos\phi \\ -(1+\sin^2\phi)/2R\sin\phi & \frac{1}{2}\cos\phi & (1+\sin^2\phi - \cos\phi)/2\sin\phi \\ 0 & 0 & 1 \end{pmatrix}$$

Radial matrix: $M_b =$ (eq. 5b)

$$\begin{pmatrix} 0 & -2R\operatorname{tg}\phi & 0 \\ 1/2R\operatorname{tg}\phi & \phi/2\operatorname{tg}\phi + 1 & 0 \\ 0 & 0 & 1 \end{pmatrix}$$

The linear magnification is given by a_{11}, the dispersion by a_{13}.

Fig. 5 summarizes the results. We did choose $\phi = 120^o$; $\beta = 16.1^o$. The principal planes, focal points and focussing distances with $R = 100$ mm can also be calculated from the matrix elements. In fig. 6 is indicated how a source-slit with a divergence of 30 millirad is imaged on the defining slit; the magnet edge is located at $\phi R = 209$ mm to the right of the source.

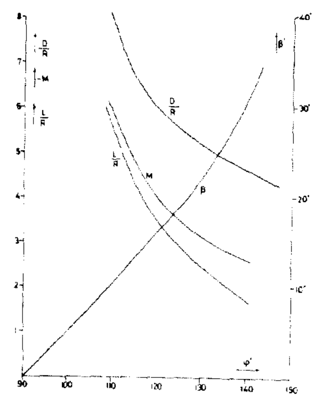

Fig. 5 - Dispersion D, magnification M, driftlength L, exit angle β, as a function of the deflection angle ϕ.

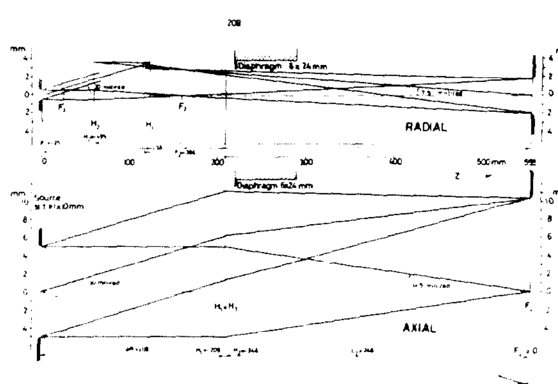

Fig. 6 - Magnet and driftlength ray tracing.

Accelerating tube and triplet. The matrix of an accelerating tube with length Z and voltage ratio $Q = \sqrt{V_2/V_1}$ is $M_q =$ (eq. 6)

$$\begin{pmatrix} (3-\sqrt{Q})/2 & 2Z\sqrt{Q}/V_2(1+\sqrt{Q}) \\ 3\sqrt{V_2}(Q-1)(1-\sqrt{Q})/8ZQ & (3\sqrt{Q}-1)/2\sqrt{Q} \end{pmatrix}$$

The principal planes and focal planes as a function of $\sqrt{Q}$ are sketched in fig. 7. The principle planes are nearly fixed at the tube entrance for a large range of voltage ratios. The mass and charge defining slit is therefore placed near the entrance of the accelerating

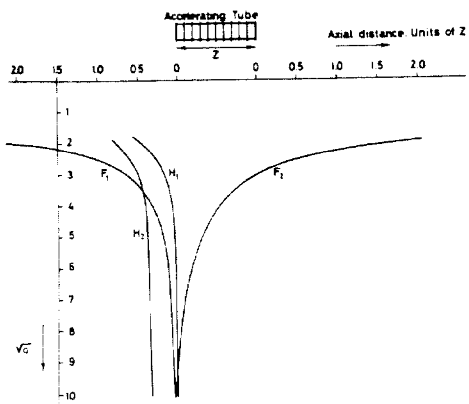

Fig. 7 - Optical characteristics of accelerator tube.

tube. Beam transport through the magnet and accelerating tube can be deduced from the product matrix. The beam radius x_e, y_e and divergence x_e' and y_e' at the exit of the tube are correlated to the radius x_s, y_s and divergence x_s' and y_s' at the source by: (eq. 7)

$$x_e = x_s(q_{11}a_{11} + q_{12}a_{21}) + x_s'(q_{12}a_{22})\sqrt{V_1} = x_sA + x_s'B$$
$$x_e' = x_s(q_{21}a_{11} + q_{22}a_{21})/\sqrt{V_2} + x_s'(q_{22}a_{22})/\sqrt{Q} = x_sC + x_s'D$$
$$y_e = y_s(q_{12}b_{21}) + y_b'(q_{11}b_{12} + q_{12}b_{22})\sqrt{V_1} = y_sE + y_s'F$$
$$y_e' = y_s(q_{22}b_{21})/\sqrt{V_2} + y_b'(q_{21}b_{12} + q_{22}b_{22})/\sqrt{Q} = y_sG + y_s'H$$

The coefficients A,B,C,D,E,F,G and H can be calculated for different values of Q. In fig. 8 four principal rays are drawn from the source through the magnet; the positions and slopes of the rays at the tube exit are calculated with eq. (7).

After the accelerating tube an electrostatic triplet is present. This triplet is not energized in fig. 8. For high Q values some rays cross the axis inside the accelerating tube. Beam diameter and divergence are small for an extraction voltage of 20 kV and a post acceleration of 320 kV (Q = 16).

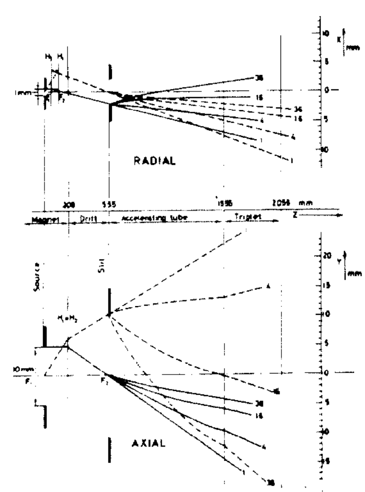

Fig. 8 - Magnet, driftlength and accelerator tube ray tracing.

Beam handling. The field edge of the magnet is chosen at 25^o instead of $\beta = 16.1^o$ to compensate for the weaker axial focussing of the magnet with a large ratio between gap and radius of curvature. A field clamp gives a sharp field cut-off. The entrance face of this clamp can be tilted to control focussing conditions. Inside the clamp are two pairs of deflection plates for beam alignment.

Moreover, the magnet with the vacuum chamber can rotate over a few degrees in the horizontal and vertical plane around the exit flange of the chamber. There are two mutual perpendicular slits each with a motor drive at the accelerating tube entrance to control the beam dimensions.

To monitor the beam a small rectangular Faraday cup can be inserted after the slit system.

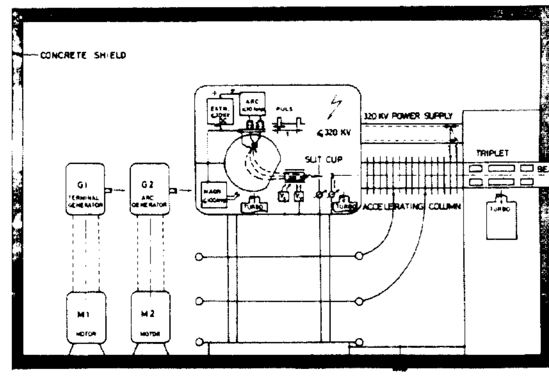

Fig. 9 - Accelerator set-up.

Vacuum system and high voltage terminal

The terminal contains two rotary pumps and two 450 l/sec turbopumps (fig. 9). A 6 × 24 mm tube with a length of 70 mm at the entrance of the field clamp forms a pumping resistance between the vacuum chamber with ion source and the slithouse with accelerating column. This arrangement combined with a third 450 l/sec turbopump at ground potential at the triplet, ensures a pressure in the lower 10^{-7} region in the accelerating column to prevent charge exchange of the ions. Titanium sublimation pumping can be combined with the two terminal turbopumps. A cut-off valve between vacuum chamber and slithouse enables ion source servicing without disturbing the tube vacuum.

All the equipment is cooled with kerosene via nylon tubes from two heat exchangers at ground potential.

Electric power is transmitted to the terminal with two 15 kVA motor-generator sets. One set is used for the source arc only, the other one for the pumps, magnet power supply and extraction supply. Motor and generator are mounted vertically with a P.V.C. tube (315 × 290 mm diameter) between the stators and a 1.1 m long P.V.C. tube (200 × 180 mm diameter) between the rotors. The resonance frequency for torsional vibration of the two stators is 140 Hz, for the two rotors 90 Hz. The lowest critical frequency for bending of the shaft is 134 Hz. All these frequencies are well above the maximum pulse repetition frequency of the ion source. A steel disc with twelve pins with rubber sleeves mounted on the motor shaft forms a flexible coupling with the P.V.C. shaft. The same construction is used at the generator side. The P.V.C. shaft is dynamically balanced before mounting. The motor is mounted via three shock-absorbers on the concrete floor.

The arc power supply consists of a rectifier with 50 µF capacitor bank, switched by a series tetrode type 4 CW 25000 A. Maximum current is 10 Amps at 10% duty-cycle and 4 kV arc voltage. Pulse duration 1 - 5 millisec. Repetition frequency 10 - 100 Hz. A 7 kV 100 µsecs pulser does ignite the arc.

The efficient and small extraction power supply makes use of a 20 kHz convertor with Cockcroft-Walton multiplier. Stabilization is by means of pulsewidth modulation of the convertor. A response time < 50 µsecs to within 0.1% of nominal value matches the pulsed beam conditions.

The accelerating voltage stack is a standard HVEC supply: 320 kV/350 µAmps.

Telemetry system

Four telemetry systems are necessary: two transmitters at ground potential control two receivers in the terminal: one receiver being at terminal voltage, the other at ion source potential equivalent to terminal plus extraction voltage.

The two other transmitters are at terminal and source potential respectively, their receivers being at ground potential in the control desk. Each transmitter-receiver coupling is established via an 8 meter long light guide with a light emitting diode at the transmitterside and a photodiode at the receiver side in a time division multiplex method. A maximum of 16 analog signals normalized to values between -10 Volt and +10 Volt is fed into an analog multiplexer. Each of the 16 signals is connected in turn for 88 μsecs to a modulus circuit generating one polarity bit and to one analog to digital converter (12 bits binary code). The total cycling time for 16 channels is 1.4 millisecs. The digital information containing 12 information bits, 4 address bits and 1 polarity bit is written in a buffermemory. From this memory content a 22 bit word is formed in a digital serializer by adding 1 start bit, 2 test bits and 2 stop bits. The start bit has a tenfold amplitude over the other bits. This large bit is used to synchronize the 10 MHz (500 kHz after frequency division) clocks in transmitter and receiver, by resetting the frequency dividing counter in the receiver. At the same time a shift register in the receiver is started by the clock. After 22 steps, the start bit passes a fixed point. If at the same time the two stop bits at the end of the word do pass two fixed points also, the word is written into a buffermemory in parallel. Each word is transmitted two times; the second word is put into a second buffermemory in the receiver. A comparator checks if the information contained in the two memories is equal. The information from one of the memories is converted in one digital to analog converter and fed into one analog demultiplexer with 16 holdcircuits. The information gate to the demultiplexer will be closed in case of a difference in the two words and an acoustical and/or optical warning signal is given to the operator.

The whole system can be tested by sending up one test bit from a transmitter at ground to a receiver in the terminal. A 5 Volt signal will then be presented to all the channels in the terminal, so all the meters in the control desk do go to half scale deflection.

A check on the transmission from various control levels (chosen with helipots on the control desk) can be performed by sending up a second test bit. In this second test the control desk meters then do show the level chosen by the helipots, because the information is sent back to earth. In both tests the hold circuits in the terminal do keep their information, so the accelerator performance is not interrupted.

The absolute accuracy of the total system is $1 \cdot 10^{-3}$; the crosstalk is less than $1 \cdot 10^{-4}$ full scale deflection at maximum amplitude in a neighbour channel. The hold circuits do reach the correct value within 0.1% in 3 cycles at maximum amplitude change; this is a compromise between accuracy and settling time. Alarm is given in case of failure of synchronism, signal distortion or transmission attenuation.

The binary code of the A/D converter can be coupled directly to the computer via a CAMAC interface. Due to the closed information gate in case of malfunctioning, false information can not reach the computer.

Analyzing magnet

The deflection angle of an ion passing through the gap of a magnet with round pole faces (diameter D) is given by:

$$\phi = 2 \text{ arc tg } D/2R \qquad \text{(eq. 8)}$$

where R is the radius of curvature in the magnetic field. If ions with energy E that are passed through a gascell change in charge state from q to n, the radius of curvature can be derived from eq. (1) for B, M and E constant. A magnet with 20 cm diameter poleshoes, with a field of 10 kGauss can be used to separate a 3500 keV Ar^{10+} ion beam after passing a gascell into ten beams with charge states 1 to 10 in a fairly regular fanout pattern; the angle between two neighbouring beams varies from 5.14° for Ar^{10+}/Ar^{9+}, to 6.73° between Ar^{+} and Ar^{0}.

Acknowledgment

This work is part of the research program of the Stichting voor Fundamenteel Onderzoek der Materie (Foundation for Fundamental Research on Matter) and was made possible by financial support from the Nederlandse Organisatie voor Zuiver-Wetenschappelijk Onderzoek (Netherlands Organization for the Advancement of Pure Research).

References

1. Saris F.W., De Heer F.J., Proceedings 4th Int.Conf. on Atomic Physics, Heidelberg, 1974.
2. Kessel Q.C., Fastrup B., Case Studies in Atomic Physics 3 (1973) 137-213.
3. Wolf B.H., IEEE Trans.Nucl.Sci. NS19, no.2 (1972) p. 74.
4. Anderson C.F., Ehlers, K.W., Rev.Sci.Instr. 27 (1956) p. 809.
5. Clark D.J., Steyart J., Carneiro A. et al., IEEE Trans.Nucl.Sci. NS18, no. 3 (1971) p.102.
NS19, no. 2 (1972) p.114.
6. Bieth C., Bourgarel M.P. et al., IEEE Trans.Nucl.Sci. NS19, no.2 (1972) p.93.
7. Septier A. (1967) "Focusing of charged particles I & II", Academic Press, New York.